nature chemistry

ARTICLES

PUBLISHED ONLINE: 14 JULY 2013 | DOI: 10.1038/NCHEM.1707

Magnetic relaxation pathways in lanthanide single-molecule magnets

Robin J. Blagg[1], Liviu Ungur[2], Floriana Tuna[1], James Speak[1], Priyanka Comar[1], David Collison[1], Wolfgang Wernsdorfer[3], Eric J. L. McInnes[1]*, Liviu F. Chibotaru[2]* and Richard E. P. Winpenny[1]*

Single-molecule magnets are compounds that exhibit magnetic bistability caused by an energy barrier for the reversal of magnetization (relaxation). Lanthanide compounds are proving promising as single-molecule magnets: recent studies show that terbium phthalocyanine complexes possess large energy barriers, and dysprosium and terbium complexes bridged by an N_2^{3-} radical ligand exhibit magnetic hysteresis up to 13 K. Magnetic relaxation is typically controlled by single-ion factors rather than magnetic exchange (whether one or more 4*f* ions are present) and proceeds through thermal relaxation of the lowest excited states. Here we report polylanthanide alkoxide cage complexes, and their doped diamagnetic yttrium analogues, in which competing relaxation pathways are observed and relaxation through the first excited state can be quenched. This leads to energy barriers for relaxation of magnetization that exceed 800 K. We investigated the factors at the lanthanide sites that govern this behaviour.

To understand the magnetism of lanthanide complexes we must first remember that the lanthanides' electronic configuration is $[Xe]4f^n5d^16s^2$, where 4*f* orbitals are internal and hence not involved in bonding to ligands or in redox processes. This makes the +3 oxidation state extremely stable, and also renders magnetic exchange between 4*f* ions very weak. For single ions the energy terms are determined by strong coupling between the spin and orbital angular moments of the ions, and then split further by crystal-field effects. This can give very large single-ion magnetic anisotropies for 4*f* ions, such as Dy^{3+} or Tb^{3+}, and has led to thermal energy barriers for the reversal of magnetization, U_{eff}, that are an order of magnitude higher than those found in *d*-block single-molecule magnets (SMMs). Such high barriers were originally reported by Ishikawa *et al.* for a terbium–phthalocyanine compound, $(Bu_4N)[Tb(Pc)_2]$ (ref. 1), with many further examples reported over the past decade[2–8].

The single-ion anisotropy has also led to extraordinary physics in $\{Dy_3\}$ triangles, where spin chirality leads to a magnetic memory effect in molecules that have a non-magnetic ground state[9,10]. The stability of the +3 oxidation states of the lanthanides allows the incorporation in complexes of unusual ligand sets, such as the N_2^{3-} radical bridge between two lanthanide centres[11,12], and to interesting magnetic behaviour of lanthanide organometallics[13], in contrast to the mainly diamagnetic *d*-block organometallics. Many ideas developed for *d*-block molecular magnets are being challenged and extended as a result of the observations made on these very different transition metals, and it also appears that 4*f* SMMs could play a major part in the development of molecular spintronics[14], with reports of molecular spin valves[15] and transistors[16].

The coordination geometry and ligand set required to observe slow magnetic relaxation are specific to each lanthanide ion. For example, for the bisphthalocyanine sandwich complexes[1,2], the terbium examples have high U_{eff}, but the erbium complexes do not behave as SMMs. In contrast, for polyoxometallate sandwich complexes[3] the opposite is the case, with the erbium complex showing the highest U_{eff}. Approaches to understanding this behaviour vary from the use of crystal-field theory[7,8] to advanced *ab initio* calculations[10,17–21].

For a 4*f* ion the ground-state total angular momentum (*J*) multiplet is split by the crystal field: for example, for Dy^{3+} the $^6H_{15/2}$ ground term splits into eight doublets which are linear combinations of $m_J = \pm 1/2 \ldots \pm 15/2$ as permitted by symmetry, where m_J is the projection of *J* on the axis of quantization. Kramers theorem states that for a half-integer *J* the states must retain at least a twofold degeneracy in zero field; hence such states are called Kramers doublets. For a lanthanide SMM the lowest energy doublet has high $|m_J|$, and the complexity of the relaxation phenomena is related to the number of relaxation paths available. First, there is a reversal mechanism via quantum tunnelling of magnetization (QTM) within the lowest energy doublet. Second, there is Orbach relaxation, which is a thermal mechanism via an excited state; this was first described by Orbach and co-workers in studies of cerium magnesium nitrate[22]. Third, there could be thermally activated QTM (TA-QTM), which occurs within an excited doublet. Previously only thermal relaxation via the first excited doublet was considered for Ln SMMs.

Here we report studies of polymetallic lanthanide alkoxide complexes and their doped yttrium analogues. We find that a strongly axial crystal field can lead to thermal relaxation via higher excited states. This leads to higher values for U_{eff}, and measurements on a $\{Dy_4K_2\}$ complex show the highest found for any polymetallic complex, and those for the Dy-doped Y complexes reach even higher energies (>800 K).

Results and discussion

Synthesis and structure. Reaction of anhydrous lanthanide (Ln) chlorides with three equivalents of potassium *tert*-butoxide in toluene, followed by crystallization from hexane, gave $[Ln_4K_2O(O^tBu)_{12}]\cdot C_6H_{14}$ (Ln = Gd, **1**·C_6H_{14}; Tb, **2**·C_6H_{14}; Dy, **3**·C_6H_{14}; Ho, **4**·C_6H_{14}; Er, **5**·C_6H_{14}) in yields of 9–46%.

[1]School of Chemistry and Photon Science Institute, The University of Manchester, Oxford Road, Manchester M13 9PL, UK, [2]Division of Quantum and Physical Chemistry, Katholieke Universiteit Leuven, Celestijenlaan 200F, 3001 Leuven, Belgium, [3]Institut Néel, Centre National de la Recherche and Université Joseph Fourier, BP 166, 38042 Grenoble Cedex 9, France. *e-mail: eric.mcinnes@manchester.ac.uk; Liviu.Chibotaru@chem.kuleuven.be; Richard.Winpenny@manchester.ac.uk

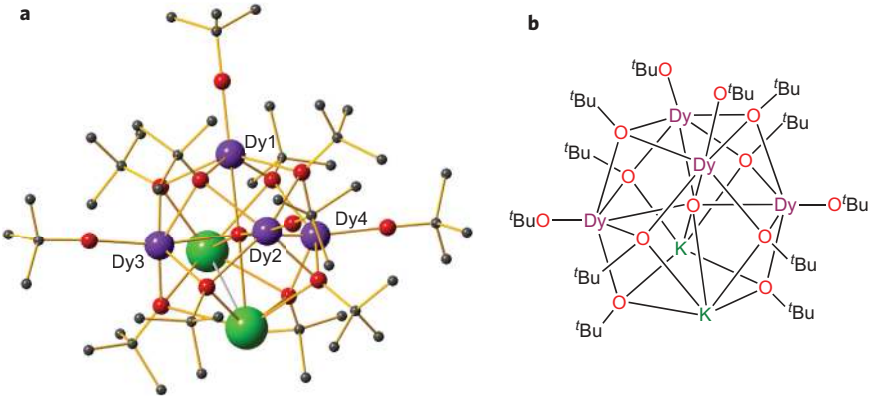

Figure 1 | The structure of $[Dy_4K_2O(O^tBu)_{12}]$ (3); compounds 1–5 are isostructural. a, The structure in the crystal. Dy, purple; K, green; O, red; C, grey (H-atoms removed for clarity). **b**, A line-drawing showing connectivity within compound 3.

Characterization by single-crystal X-ray diffraction showed the compounds to be isostructural (Fig. 1; see Supplementary Section 2.0 for selected structural parameters, including bond lengths and angles).

In 3 the four Dy ions and two K ions form an oxo-centred octahedron with a *cis* arrangement of the two potassiums. As a result, two of the lanthanide ions (Dy1 and Dy2 in Fig. 1) are *trans* to a potassium ion and distinct from the other two (Dy3 and Dy4), which are mutually *trans*. Each face of the $\{Dy_4K_2\}$ octahedron is bridged by a μ_3-O^{t}Bu ligand and there is a terminal *tert*-butoxide on each lanthanide centre. There are no terminal ligands on the potassium ions, although there are intramolecular K···H agostic interactions ($2.62 < K\cdots H < 3.30$ Å) with adjacent O^{t}Bu groups.

The Dy sites are six coordinate, with distorted octahedral geometries. The Dy is displaced from the plane formed by the four μ_3-O(^{t}Bu), towards the terminal butoxide and away from the central μ_6 oxide, with Dy–O bond lengths 0.2–0.3 Å shorter to the terminal butoxides than to the μ_6 oxide. There is also a statistically significant difference in the Dy–(μ_6O) distances for the Dy1,2 and the Dy3,4 sites, being around 0.06 Å shorter for the former.

Magnetic measurements. Magnetic measurements were performed on 1–5. We focus on the $\{Dy_4K_2\}$ compound 3, as this shows by far the most interesting relaxation properties (Fig. 2). Direct current (d.c.) measurements tell us about the static magnetic behaviour of the compounds. The room temperature value for χ_mT (where χ_m is the molar magnetic susceptibility, that is the rate of magnetization in an external magnetic field, and T is the temperature) is close to the predicted value for four independent Dy(III) ions (measured, 56.34 cm^3 K mol^{-1}; calculated, 56.68 cm^3 K mol^{-1}). On cooling, χ_mT decreases gradually until 30 K, and then more rapidly, owing to single-ion crystal-field effects (see later). The low-temperature magnetization (M) against applied magnetic field (H) saturates at 21.43 μ_B at 70 kG and 1.8 K (Supplementary Fig. S3). These results are entirely normal and show that any Dy···Dy interactions must be very weak or absent.

In contrast, alternating current (a.c.) measurements tell us about dynamic processes, such as relaxation of magnetization, which show an unusual and complex behaviour. There are two distinct thermal relaxation processes, as shown by two distinct frequency-dependent peaks at high temperature for the out-of-phase susceptibility χ_m'' (at about 30 and 47 K for a frequency (ν) of 1.2 kHz) (Fig. 2a and Supplementary Fig. S4). Plots of χ_m'' against in-phase susceptibility χ_m' (Cole–Cole plots) are also in good agreement with this (Fig. 2b). An Arrhenius plot of these data (Fig. 2d), which shows the temperature dependence of the magnetic relaxation time (τ), gives $U_{eff} = 692$ and 316 K with pre-exponential factors $\tau_0 = 6.6 \times 10^{-11}$ and 2.6×10^{-9} s, respectively, which fall in the range for lanthanide-based SMMs. Fitting the Cole–Cole plots to two modified Debye functions to determine relaxation times gave small distributions ($0.03 < \alpha_{692} < 0.08$; $0.16 < \alpha_{316} < 0.31$ where an α value of 0 would be no distribution).

These characteristics can be compared to those obtained from previous studies for a related complex, $[Dy_5O(O^iPr)_{13}]$ (6), for which a single peak in $\chi_m''(T)$ was observed and gave a thermal energy barrier for the reversal of magnetization of $U_{eff} = 528$ K with $\tau_0 = 4.7 \times 10^{-10}$ s (ref. 23). The $\{Dy_5\}$ square-pyramidal structure of 6 (centred on a μ_5 oxide) is clearly related to the $\{Dy_4K_2\}$ octahedron of 3 (Fig. 3), with very similar Dy coordination geometries: a short terminal alkoxide *trans* to the central oxide, and four 'equatorial' μ alkoxides.

We investigated the effect of magnetic dilution on the relaxation of magnetization to test the influence of inter- and intramolecular exchange on the magnetic behaviour[24,25]. To this end, we prepared the isostructural and diamagnetic yttrium analogues of 3 and 6, $[Y_4K_2O(O^tBu)_{12}]$ (7) and $[Y_5O(O^iPr)_{13}]$ (8) (see Supplementary Section 1.0). We doped these materials in two ways:

(1) We co-crystallized preformed 3 or 6 (~5%) with the appropriate yttrium complex, hence magnetically isolating the $\{Dy_4K_2\}$ or $\{Dy_5\}$ cages in the solid state; we found little change in the a.c. magnetic behaviour from pure 3 and 6, and hence intermolecular interactions do not affect the thermal relaxation behaviour of these materials.
(2) We incorporated a small amount of $DyCl_3$ (~5%) in the synthesis of 7 and 8 to give $\{DyY_3K_2\}$ in a $\{Y_4K_2\}$ matrix or $\{DyY_4\}$ in $\{Y_5\}$; we label these Dy@7 and Dy@8, respectively.

For Dy@7 and Dy@8, in which the individual Dy ions are magnetically isolated, there are stark changes. In both cases a single dominant relaxation process was observed in both $\chi_m''(T)$ and $\chi_m''(\nu)$ (Fig. 2 and Supplementary Figs S5 and S6), with the out-of-phase response surviving to significantly higher temperatures. The values of U_{eff} determined from the Arrhenius treatment of these data are 842 K for Dy@7 (Fig. 2d) and 804 K for Dy@8. These values of U_{eff} are among the highest reported for any SMM.

Electronic structure calculations. We performed *ab initio* CASSCF calculations on 3–6, Dy@7 and Dy@8 with MOLCAS 7.8 (see Supplementary Section 4.0 for details), a method that is successful in interpreting the magnetism of lanthanide complexes[10,19,20]. The calculations reproduce well the d.c. magnetic measurements of 3–6 (Supplementary Figs S14–S16 and S19–S21). Modelling the effect of surrounding molecules by including Madelung fields makes no significant difference to the electronic structure, as might be expected (Supplementary Tables S10–S15).

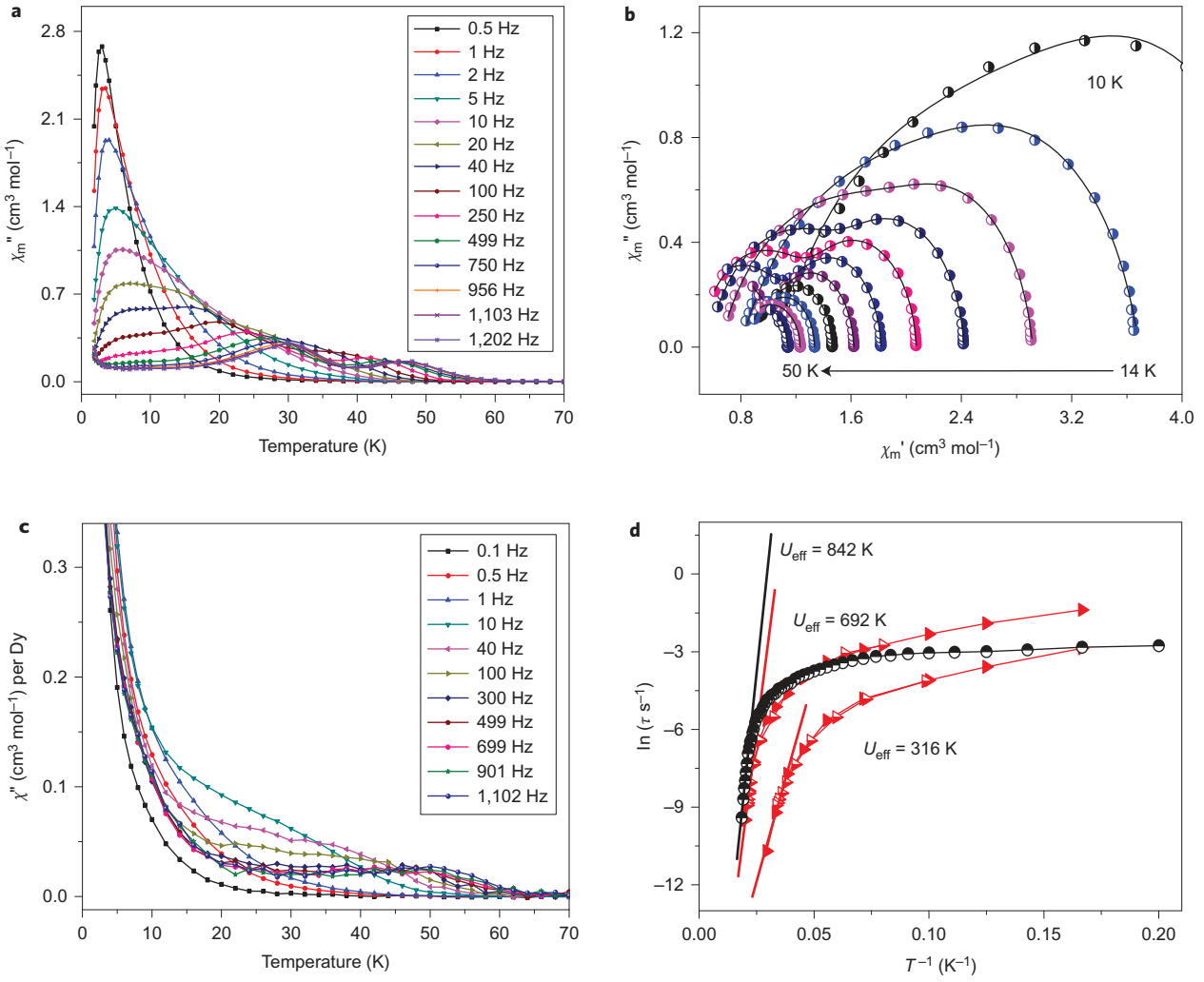

Figure 2 | Magnetic measurements on {Dy_4K_2} (3) and Dy in {Y_4K_2} Dy@7. a, $\chi_m''(T)$ for **3** measured in the frequency range 0.1–1.2 kHz, in zero d.c. field and 1.55 Oe a.c. field. **b**, Plots of χ_m'' against χ_m' for **3** showing two distinct thermal relaxation processes fitted with two modified Debye functions. **c**, $\chi_m''(T)$ for Dy@**7** under the same conditions. **d**, Arrhenius treatment of χ_m'' data for the two high-temperature processes in **3** (red triangles) and the single process in Dy@**7** (black circles); the energy barriers derived from the linear high-temperature part of the curves are also given.

For each Dy site in **3** and **6** the ground Kramers doublet (labelled as states 1+ and 1− in Fig. 3a, referred to as 1±) is calculated to be essentially pure, $m_J = \pm 15/2$, with effective g values of $g_z \approx 20$ and $g_{x,y} \approx 0$ (see Supplementary Table S11; the effective g values describe the splitting of the two components of the Kramers doublet in a magnetic field). The doublet therefore has zero magnetic moment in the xy plane, that is, it is an ideal Ising state.

The magnetic moment lies entirely along the z-axis, and is as large as possible for Dy^{3+}; the z-axis is coincident with the oxide–Dy–terminal alkoxide axis for all Dy sites (Fig. 3b,c and Supplementary Table S12). The first excited Kramers doublet (state 2±) is also almost a pure Ising state with $m_J = \pm 13/2$ ($g_z \approx 17$, $g_{x,y} < 0.5$), and in this state the magnetic moment also lies along the oxide–Dy–terminal alkoxide axis for each site. The second excited Kramers doublet (state 3±) is the lowest energy state with a substantial transverse magnetic moment ($g_z \approx 12$–16, $g_{x,y} < 4$), which is associated with scrambling of the m_J functions.

For the Dy sites in **3**, the average calculated energy gaps to the 2± and 3± states are 536 and 888 K, respectively (Supplementary Table S9). For the Dy sites in **6**, the equivalent values are 576 and 986 K. The experimental U_{eff} barriers (>800 K) for Dy@**7** and Dy@**8** are much too large for relaxation via the state 2±, and must be associated with the state 3±. Hence, relaxation via the first Kramers doublet is quenched, or at least uncompetitive, in both dilute compounds. We discuss the undiluted compounds later.

There are two explanations for the preferential relaxation via state 3± in Dy@**7** and Dy@**8**. First, the TA-QTM mechanism via state 2± is suppressed because of the very small transverse g values. Second, Orbach relaxation via state 2± is blocked because, for each Dy site, states 1± and 2± are not only Ising like, but their principal axes of magnetization (g_z) are almost parallel (Fig. 3 and Supplementary Table S9). As discussed elsewhere[19], a significant non-coincidence between different Kramers doublets enhances Orbach relaxation. For example, in Powell and Sessoli's {Dy_3} triangle, where this angle is 42°, the magnetic moment's matrix elements connecting pairs of states (for example, 1− , 2+ and 2− , 1+ in Fig. 3a) with opposite directions of magnetization are of the order of 10^{-1} μ_B (ref. 19). This enhances Orbach relaxation via a single common state (for example, 1− → 2− → 1+ in Fig. 3a). In contrast, for the Dy sites in **3** and **6**, where the non-coincidence angle <3° (Supplementary Table S9), the equivalent matrix elements are several orders of magnitude smaller (Supplementary Table S22), which greatly reduces the probability of relaxation via this pathway. The increased transverse moments in state 3± lead to much larger matrix elements connecting states (3− , 3+) and (3− , 2+). These two reasons lead to processes via

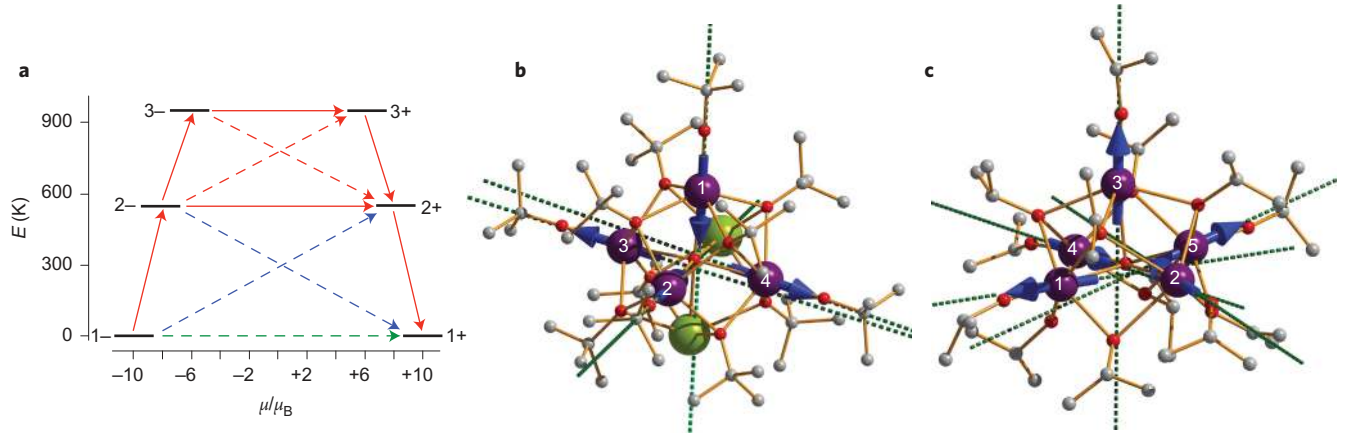

Figure 3 | Low-lying electronic structure for 3 and 6. a, Lowest three Kramers doublets for individual Dy sites, and possible relaxation paths (indicative energies). The thick black lines represent the Kramers doublets as a function of their magnetic moment along the main anisotropy axis. The green dashed line corresponds to ground-state QTM, and the solid red lines to TA-QTM via the first and second excited Kramers doublets. Dashed red and blue lines show possible Orbach processes. **b**,**c**, Calculated orientations of the principal magnetic axes in $\{Dy_4K_2\}$ (**3**) and $\{Dy_5\}$ (**6**), respectively. Arrows show the local magnetic moments in the ground Kramers doublets (see Supplementary Section 4.0).

the doublet $3\pm$ becoming dominant, and thus explain why we see the U_{eff} corresponding to the second excited Kramers doublet in the magnetically dilute compounds.

The different behaviours of the undiluted samples **3** and **6** are a consequence of the intramolecular interactions with neighbouring dysprosium atoms, which create significant local fluctuating transverse magnetic fields. As a result, the tunnel splitting within the $\pm m_J$ Kramers doublets (proportional to the transverse component of H) is also much larger, making relaxation via TA-QTM through $(2-, 2+)$ more competitive. Increased tunnel splitting will also make ground-state QTM more competitive at all temperatures. Hence, in the thermal regime we see U_{eff} corresponding to the first excited Kramers doublet, the first available thermal relaxation pathway, but this U_{eff} is lower than predicted by electronic structure calculations because QTM is not completely suppressed.

U_{eff} as derived from the slope of the high-temperature $\ln(\tau)$ versus $1/T$ data is often smaller than expected from calculated Kramers doublet energies because this simple analysis assumes exclusively thermal processes and hence neglects relaxation via ground-state QTM. We stress that U_{eff} is an effective barrier; although relaxation curves (Fig. 2d and Supplementary Fig. S8) appear as straight lines in some temperature regions, they reflect a combination of several relaxation processes with different temperature dependences.

It is already demonstrated that both magnetic dilution of samples[25] and application of a moderate d.c. magnetic field[26] suppress ground-state QTM, and result in an increase of U_{eff}, for example in a $\{Dy_3\}$ triangle, from 36 to 120 K (ref. 26). Here we see the same principle in operation; in the pure compounds **3** and **6** QTM is not completely suppressed because the Dy···Dy distances are only a little over 3.4 Å (Supplementary Table S4), and hence the measured U_{eff} is lowered. In the doped compounds dipolar interactions are reduced and hence QTM is suppressed, and U_{eff} is much closer to the value predicted by electronic structure calculations. QTM is also suppressed in the thermal regime in some monometallic Ln polyoxometallates[27] in which there are relatively large distances (>13 Å) between paramagnetic centres. However, in many systems QTM remains competitive even in the regime where thermal relaxation is dominant.

This still requires an explanation as to why we observe exclusively relaxation via state $2\pm$ in **6**, but that relaxation via $3\pm$ (TA-QTM or Orbach relaxation) remains competitive for **3**, as witnessed by the two peaks in $\chi_m''(T,\nu)$. As the Ising magnetic moments lie along the Dy–oxide axes, for any given Dy site only neighbouring Dy ions in a *cis* position (with respect to the central oxide) contribute to the transverse field it experiences. In the square-pyramidal $\{Dy_5\}$ **6**, all positions have either four (Dy3, the apex) or three (Dy1,2,4,5) *cis* Dy neighbours. In the octahedral $\{cis\text{-}Dy_4K_2\}$ **3**, Dy1,2 have three *cis* Dy neighbours but Dy3,4 have only two. Hence the internal transverse fields at Dy1,2 in **3** will be similar to the bulk of the sites in **6**, which leads to relaxation via state $2\pm$. At sites Dy3,4 the transverse fields must be markedly weaker, and may be insufficient to make relaxation via state $2\pm$ more favourable than relaxation via $3\pm$. These conclusions are supported by the calculated transverse fields on Dy ions generated by their Dy neighbours (Supplementary Table S19). Moreover, the longer Dy–oxide distances for Dy3,4 compared to Dy1,2 give weaker crystal fields and hence lower energy gaps to state $3\pm$ (Supplementary Table S9), which also keeps the $3\pm$ pathways more competitive for Dy3,4 in compound **3**. Such an analysis requires that the structurally distinct sites in $\{Ln_4K_2\}$ are more magnetically distinct than the structurally distinct sites in $\{Ln_5\}$. This is supported by solid-state ^{89}Y NMR spectroscopy of **7** and **8**. For **7** two peaks (1:1 intensity) are observed, at +180 and +200 ppm; for **8** there are two overlapping peaks (4:1), with much closer chemical shifts of +230 and +238 ppm, respectively.

The chemical dilution also has a significant effect on low-temperature magnetization against applied field behaviour (Fig. 4 and Supplementary Figs S7 and S8). For pure **3**, narrow $M(H)$ loops are observed up to ~5 K for field sweep rates of above ~0.14 T s^{-1}, as monitored by micro-SQUID (superconducting quantum interference devices) measurements on a single crystal (Fig. 4a).

There is no significant QTM step at 0 T, with a step instead seen at around 0.2 T, which we attribute to exchange biasing of the quantum tunnelling, similar to examples reported previously[28–30]. The exchange biasing of the QTM is also seen in the Arrhenius plot (Fig. 2d), which shows that a thermal contribution to relaxation still occurs even at the lowest temperatures. For Dy@**7**, broader $M(H)$ loops are seen even for field sweep rates as low as 0.001 T s^{-1} and temperatures as high as 6 K. There is now a very sharp step at 0 T as the QTM becomes dominant at these low temperatures. This is seen clearly in the Arrhenius plot (Fig. 2d), in which the relaxation becomes temperature independent, indicating we are in a pure quantum regime (without any thermal process). Compound **6** shows very similar behaviour to that of compound **3** (Supplementary Fig. S8); for Dy@**8**, hysteresis is observed in the

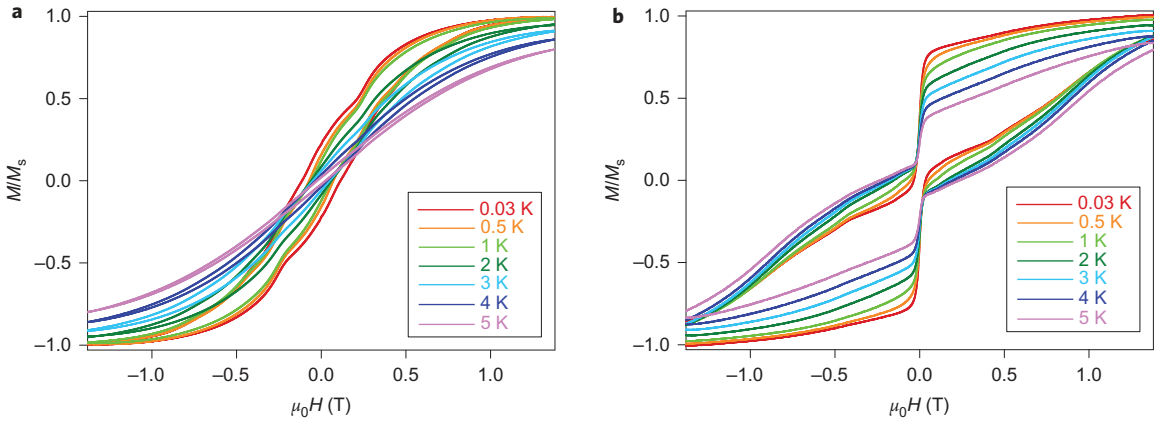

Figure 4 | Single-crystal measurements of *M*(*H*) measured on a micro-SQUID array. a,**b**, Measured at a sweep rate of 0.14 T s^{-1} at temperatures from 0.03 to 5 K for **3** (**a**) and for Dy@**7** (**b**).

M(*H*) loops to 5 K, but are narrower than in Dy@**7**. There is a large step at 0 T, but the Arrhenius plot (Supplementary Fig. S8) does not become temperature independent, which indicates that some thermal process is still operative at 5 K. The difference between Dy@**7** and Dy@**8** is a subject for further investigation.

As far as we are aware, this is the first observation of preferential relaxation via the second excited Kramers doublet in a lanthanide SMM. Competitive Orbach relaxation via two low-lying Kramers doublets (23 and 29 K) was discussed for the non-molecular $Dy(H_2O)_9(EtOSO_3)_3$ salt[31], but not the switching off of the lowest energy process, and clearly the energy scales here are vastly different (<30 K versus >800 K). In the lanthanide ethylsulfates the relaxation is via the absorption of acoustic phonons (energies up to around 30–40 K) and is described simply by the Debye model; this is also the case in classic *d*-block SMMs such as $\{Mn_{12}\}$ and $\{Fe_8\}$ (ref. 32). For the Dy ions in **3**, **6**, Dy@**7** and Dy@**8** the gaps are many hundred Kelvins, and the spin–vibrational transitions must involve optical phonons (energies up to around 300–400 K) and multiphonon absorption.

The *ab initio* calculations on other members of the $\{Ln_4K_2\}$ family also fit with experiment (Supplementary Table S23 and Supplementary Figs S19–S21). We found that the Ho complex **4** also has a highly axial magnetic structure at each site (Supplementary Table S24), but the tunnel splittings for the ground doublet (Supplementary Table S28) are large for this non-Kramers ion. Experimentally, we found slow relaxation up to ~30 K from $\chi_m''(T,\nu)$, with the peak in $\chi_m''(T)$ being severely broadened (Supplementary Fig. S9) and with incomplete semicircular Cole–Cole plots (found up to 20 K; Supplementary Fig. S10). Arrhenius analysis of $\chi_m''(\nu)$ gives U_{eff} of about 90 K, which is a substantial thermal barrier, but lower than that for its Dy analogue **3** and is consistent with the behaviour of **6** and its Ho analogue[23,33]. For the Er complex **5**, the calculations show that the magnetic structure at the individual Er ions is not axial (Supplementary Table S24), and the tunnel splitting of the lowest exchange doublets is non-negligible (Supplementary Table S29), and hence this compound should not behave as an SMM and experimentally we do not observe any frequency-dependent magnetic behaviour down to 1.8 K.

Conclusion

The U_{eff} values for the diluted complexes Dy@**7** and Dy@**8** are higher than those reported for any SMM, other than a very recent report of a heteroleptic Tb phthalocyanine complex (U_{eff} = 938 K)[34]. More importantly, the results show that in lanthanide SMMs it is possible to block relaxation via the first excited state, which leads to higher energy barriers. The key feature is a strong axial ligand field that maximizes the gaps between $|m_J|$ states, and thus minimizes the mixing between them and enforces the co-parallel alignment of the anisotropy axes of the lowest Kramers doublets even where, as here, there is no symmetry.

Lanthanide ions tend to have high coordination numbers, and even where there is symmetry (for example, tricapped trigonal prisms or square anti-prisms) there are few[21,27] if any donor atoms on the symmetry axis. In the materials discussed here we have a tetragonally distorted octahedral crystal field and this is the dominant factor in deciding the thermal energy barrier, rendering the strict point-group symmetry at the lanthanide sites less important. Our analysis also suggests that minor changes in the structure could switch relaxation paths on and off, and hence minor external perturbations could produce dramatic changes in energy barriers.

Received 25 April 2013; accepted 11 June 2013;
published online 14 July 2013

References

1. Ishikawa, N., Sugita, M., Ishikawa, T., Koshihara, S-Y. & Kaizu, Y. Lanthanide double-decker complexes functioning as magnets at the single-molecular level. *J. Am. Chem. Soc.* **125,** 8694–8695 (2003).
2. Takamatsu, S., Ishikawa, T., Koshihara, S-Y. & Ishikawa, N. Significant increase of the barrier energy for magnetization reversal of a single-4*f*-ionic single-molecule magnet by a longitudinal contraction of the coordination space. *Inorg. Chem.* **46,** 7250–7252 (2007).
3. AlDamen, M. A. *et al.* Mononuclear lanthanide single molecule magnets based on the polyoxometalates $[Ln(W_5O_{18})_2]^{9-}$ and $[Ln(\beta_2\text{-}SiW_{11}O_{39})_2]^{13-}$ (Ln^{III} = Tb, Dy, Ho, Er, Tm, and Yb). *Inorg. Chem.* **48,** 3467–3479 (2009).
4. Habib, F. *et al.* Supramolecular architectures for controlling slow magnetic relaxation in field-induced single-molecule magnets. *Chem. Sci.* **3,** 2158–2164 (2012).
5. Woodruff, D. N., Winpenny, R. E. P. & Layfield, R. A. Lanthanide single-molecule magnets. *Chem. Rev.* http://dx.doi.org/10.1021/cr400018q (2013).
6. Jiang, S-D. *et al.* Series of lanthanide organometallic single-ion magnets. *Inorg. Chem.* **51,** 3079–3087 (2012).
7. Sorace, L., Benelli, C. & Gatteschi, D. Lanthanides in molecular magnetism: old tools in a new field. *Chem. Soc. Rev.* **40,** 3092–3104 (2011).
8. Baldoví, J. J., Borrás-Almenar, J. J., Clemente-Juan, J. M., Coronado, E. & Gaito-Ariño, A. Modelling the properties of lanthanoid single-ion magnets using an effective point-charge approach. *Dalton Trans.* **41,** 13705–13710 (2012).
9. Tang, J. K. *et al.* Dysprosium triangles showing single-molecule magnet behavior of thermally excited spin states. *Angew. Chem. Int. Ed.* **45,** 1729–1733 (2006).
10. Chibotaru, L. F., Ungur, L. & Soncini, A. The origin of nonmagnetic Kramers doublets in the ground state of dysprosium triangles: evidence for a toroidal magnetic moment. *Angew. Chem. Int. Ed.* **47,** 4126–4129 (2008).
11. Rinehart, J. D., Fang, M., Evans, W. J. & Long, J. R. Strong magnetic exchange and magnetic blocking in N_2^{3-} radical-bridged lanthanide complexes. *Nature Chem.* **3,** 538–542 (2011).
12. Rinehart, J. D., Fang, M., Evans, W. J. & Long, J. R. A N_2^{3-} radical-bridged terbium complex exhibiting magnetic hysteresis at 14 K. *J. Am. Chem. Soc.* **133,** 14236–14239 (2011).

13. Layfield, R. A., McDouall, J. J. W., Sulway, S. A., Tuna, F. & Winpenny, R. E. P. Influence of the N-bridging ligand in dimetallic organometallic dysprosium single molecule magnets. *Chem. Eur. J.* **16,** 4442–4446 (2010).
14. Katoh, K., Isshiki, H., Komeda, T. & Yamashita, M. Molecular spintronics based on single-molecule magnets composed of multiple-decker phthalocyaninato terbium(III) complex. *Chem. Asian J.* **7,** 1154–1169 (2012).
15. Urdampilleta, M., Cleuziou, J-P., Klyatskaya, S., Ruben, M. & Wernsdorfer, W. Supramolecular spin valves. *Nature Mater.* **10,** 502–506 (2011).
16. Vincent, R., Klyatskaya, S., Ruben, M, Wernsdorfer, W. & Balestro, F. Electronic read-out of a single nuclear spin using a molecular spin transistor. *Nature* **488,** 357–360 (2012).
17. Petit, S., Pilet, G., Luneau, D., Chibotaru, L. F. & Ungur, L. A dinuclear cobalt(II) complex of calix[8]arenes exhibiting strong magnetic anisotropy. *Dalton Trans.* **40,** 4582–4588 (2007).
18. Chibotaru, L. F. *et al.* Structure, magnetism and theoretical study of a mixed-valent $Co^{II}_3Co^{III}_4$ heptanuclear wheel: lack of SMM behaviour despite negative magnetic anisotropy. *J. Am. Chem. Soc.* **130,** 12445–12455 (2008).
19. Ungur, L. & Chibotaru, L. F. Magnetic anisotropy in the excited states of low symmetry lanthanide complexes. *Phys. Chem. Chem. Phys.* **13,** 20086–20090 (2011).
20. Mondal, K-C. *et al.* Evidence for coexistence of distinct single-ion and exchange-based mechanisms for blocking of magnetization in a $Co^{II}_2Dy^{III}_2$ single molecule magnet. *Angew. Chem. Int. Ed.* **51,** 7550–7554 (2012).
21. Cucinotta, G. *et al.* Magnetic anisotropy in a dysprosium/DOTA single-molecule magnet: beyond simple magneto-structural correlations. *Angew. Chem. Int. Ed.* **51,** 1606–1610 (2012).
22. Finn, C. B. P., Orbach, R. & Wolf, W. P. Spin-lattice relaxation in cerium magnesium nitrate at liquid helium temperature: a new process. *Proc. Phys. Soc.* **77,** 261–268 (1961).
23. Blagg, R. J., Muryn, C. A., McInnes, E. J. L., Tuna, F. & Winpenny, R. E. P. Single pyramid magnets: Dy_5 pyramids with slow magnetic relaxation to 40 K. *Angew. Chem. Int. Ed.* **50,** 6530–6532 (2011).
24. Luis, F. *et al.* Spin-lattice relaxation via quantum tunnelling in an Er^{3+} polyoxometallate single molecule magnet. *Phys. Rev. B* **82,** 060403 (2010).
25. Meihaus, K. R., Rinehart, J. D. & Long, J. R. Dilution-induced slow magnetic relaxation and anomalous hysteresis in trigonal prismatic dysprosium(III) and uranium(III) complexes. *Inorg. Chem.* **50,** 8484–8489 (2011).
26. Luzon, J. *et al.* Spin chirality in a molecular dysprosium triangle: the archetype of the noncollinear Ising model. *Phys. Rev. Lett.* **100,** 247205 (2008).
27. Cardona-Serra, S. *et al.* Lanthanoid single-ion magnets based on polyoxometallates with a 5-fold symmetry. The series $[LnP_5W_{30}O_{110}]^{12-}$ (Ln^{3+} = Tb, Dy, Ho, Er, Tm and Yb). *J. Am. Chem. Soc.* **134,** 14982–14990 (2012).
28. Long, J. *et al.* Single-molecule magnet behaviour for an anti-ferromagnetically superexchange-coupled dinuclear dysprosium(III) complex. *J. Am. Chem. Soc.* **133,** 5319–5328 (2011).
29. Guo, Y-N. *et al.* Strong axiality and Ising exchange interaction suppresses zero-field tunneling of magnetization of an asymmetric Dy_2 single-molecule magnet. *J. Am. Chem. Soc.* **133,** 11948–11951 (2011).
30. Sulway, S. A., Layfield, R. A., Tuna, F., Wernsdorfer, W. & Winpenny, R. E. P. Single-molecule magnetism in cyclopentadienyl-dysprosium chlorides. *Chem. Commun.* **48,** 1508–1510 (2012).
31. Van den Broek J. & Van der Marel, L. C. Spin-lattice relaxation in rare earth ethylsulphates II. *Physica* **30,** 565–587 (1964).
32. Garanin, D. A. & Chudnovsky, E. M. Thermally activated resonant magnetization tunnelling in molecular magnets: $Mn_{12}Ac$ and others. *Phys. Rev. B* **56,** 11102–11118 (1997).
33. Blagg, R. J., Tuna, F., McInnes, E. J. L. & Winpenny, R. E. P. Pentametallic lanthanide-alkoxide square-based pyramids: high energy barrier for thermal relaxation in a holmium single molecule magnet. *Chem. Commun.* **47,** 10587–10589 (2011).
34. Ganivet, C. R. *et al.* Influence of peripheral substitution on the magnetic behaviour of single-ion magnets based on homo- and heteroleptic Tb^{III} bis(phthalocyaninate). *Chem. Eur. J.* **19,** 1457–1465 (2013).

Acknowledgements

This work was supported by the Engineering and Physical Sciences Research Council (UK), by the Flemish Science Foundation (fellowship to L.U.) and by the European Research Council Advanced Grant MolNanoSpin (number 226558) and ICT-2007.8.0 Future Emerging Technologies Open, Quantum Information Processing Specific Targeted Research Project number 211284 MolSpinQIP. R.E.P.W. thanks The Royal Society for a Wolfson research merit award, and financial support from the Institute for Nanoscale Physics and Chemistry and Methusalem programs at KU Leuven is gratefully acknowledged. We also acknowledge Diamond Light Source for access to synchrotron X-radiation.

Author contributions

E.J.L.M., D.C. and R.E.P.W. designed the research. R.J.B., P.C. and J.S. made the compounds; R.J.B. also carried out the X-ray studies. L.U. and L.F.C. performed the *ab initio* calculations and proposed the interpretation. F.T. and W.W. performed the magnetic measurements. E.J.L.M., D.C. and R.E.P.W. co-wrote the paper with input from all other authors.

Additional information

Supplementary information and chemical compound information are available in the online version of the paper. Reprints and permissions information is available online at www.nature.com/reprints. Correspondence and requests for materials should be addressed to E.J.L.M., L.F.C. and R.E.P.W.

Competing financial interests

The authors declare no competing financial interests.